Journal of Alloys and Compounds 887 (2021) 161334

Contents lists available at ScienceDirect

Journal of Alloys and Compounds

journal homepage: www.elsevier.com/locate/jalcom

Effects of recovery and recrystallization on microstructure and texture during annealing of a cold deformed superconducting Nb-50(wt.)%Ti alloy

Andrei Marx Ferreira[a], Marcelo Aquino Martorano[a,*], Nelson Batista de Lima[b], Angelo Fernando Padilha[a]

[a] Department of Metallurgical and Materials Engineering, University of São Paulo, Av. Prof. Mello Moraes, 2463, São Paulo, SP 05508-030, Brazil
[b] Department of Materials Characterization, Nuclear and Energy Research Institute (IPEN), Av. Prof. Lineu Prestes, 2242, São Paulo, SP 05508-900, Brazil

ARTICLE INFO

Article history:
Received 11 April 2021
Received in revised form 22 July 2021
Accepted 24 July 2021
Available online 27 July 2021

Keywords:
Nb-50Ti alloy
Recovery
Recrystallization
Curly structure
Texture

ABSTRACT

A Nb-50(wt.)%Ti alloy was melted and remelted in an electron beam furnace and the cast ingot was subsequently deformed into a bar by cold swaging, undergoing a maximum reduction in the area of 90%. Samples of the cold deformed bar were subjected to isochronous annealing cycles for 1 h in the temperature range between 250 and 1000 °C. The microstructural changes of the samples were monitored by optical microscopy, scanning electron microscopy with backscattered electron diffraction (EBSD), X-ray diffraction for pattern and texture determinations, and Vickers microhardness measurements. Recovery is the main softening mechanism in the samples annealed at temperatures up to 600 °C, but recrystallization is significant at temperatures equal to or above 750 °C and might also contribute to softening. Grain growth is also noted after annealing at the temperatures of 900 °C and 1000 °C. The microstructures of the cold deformed sample and of the samples annealed at temperatures up to 600 °C display a curly structure caused by deformation bands and their dislocation substructures. At the annealing temperatures of 900 °C and 1000 °C, complete recrystallization occurs and eliminates the deformation bands, but the curly pattern still exists and is probably due to a residue of the microsegregation of elements that occurs during solidification of the ingot. An intense fiber texture that is typical of cold swaging is observed in the cold deformed sample and in those annealed at temperatures up to 750 °C, but annealing at temperatures of 900 °C and 1000 °C weakens this texture owing to complete recrystallization. The results of the present work show the importance of the strong interactions among the phenomena of recovery, recrystallization, and microsegregation in determining the microstructure and texture of cold deformed and annealed Nb-Ti alloys.

1. Introduction

The main application of Nb is as an alloying element added to melts of steels and superalloys in the form of Fe-Nb or Ni-Nb alloys, produced by aluminothermic reduction. Pure Nb, Nb alloys, and Nb compounds have applications that are more specific and are produced in smaller quantities and sold at higher prices. Pure Nb is superconducting at very low temperatures, but several Nb compounds (Nb_3Sn, Nb_3Al, Nb_3Ga, and Nb_3Ge) and Nb solid solutions (Nb-Ti, Nb-Zr) have better superconducting properties [1,2]. The alloys of the Nb-Ti system are the most largely produced Nb alloys and are used in superconducting cables, electromagnets, and orthopedic/orthodontic implants [3–8]. Superconducting commercial Nb-Ti alloys, generally with Ti contents between 45 and 65 (wt.)%, display a unique combination of critical temperature, critical current, and critical magnetic field [7,9]. Although these alloys are essentially solid solutions with a body-centered cubic crystalline structure, other phase structures may form below 600 °C for higher Ti contents [10,11].

In general, the production of Nb-Ti ingots starts with melting and eventually remelting in a vacuum arc remelting (VAR) furnace. An alternative processing step is the electron beam melting (EBM), with the important advantage of a relatively low final concentration of interstitial elements (C, N, O, and H), improving ductility, toughness, and superconducting properties [12,13]. Important disadvantages of

* Corresponding author.
E-mail addresses: andrei.marx@usp.br (A.M. Ferreira), martoran@usp.br (M.A. Martorano), nblima@ipen.br (N.B. de Lima), padilha@usp.br (A.F. Padilha).

https://doi.org/10.1016/j.jallcom.2021.161334
0925-8388/

the EBM process, however, are the difficult control of chemical composition due to evaporation of Ti during melting under high vacuum and the microsegregation of elements during solidification in a water-cooled copper mold [14].

A possible subsequent processing step of the Nb-Ti alloys is the plastic deformation of their cast ingots. Because of their very good manufacturability and ductility, bars of these alloys with diameters of several centimeters are plastically deformed into superconducting filaments with micrometric diameters for the production of superconducting cables [15]. During cold deformation of these alloys, curly grain patterns observed in other refractory metals and alloys [16,17] and named van Gogh sky (VGS) microstructures can also form.

Intermediate annealing cycles are often required during mechanical processing, causing precipitation of phases, recovery, and recrystallization, which might significantly change the microstructure of the deformed alloy [18] and its superconducting properties [19,20]. As an example, precipitates and subgrain boundaries formed during recovery would work as flux pinning centers and improve superconducting properties [19,20].

Recovery and recrystallization studies of Nb-Ti alloys produced by EBM and subsequently cold deformed by swaging are very scarce in the scientific literature. For example, the competition between recovery and recrystallization during annealing and the interactions between microsegregation and the curly structure in these alloys have not yet been studied in detail [21,22]. Particularly the Nb-50(wt.)%Ti alloy is the least studied among all the superconducting Nb-Ti alloys [14,21].

The main objective of this work is to study the microstructural modifications during isochronous annealing cycles of 1 h at temperatures between 250 °C and 1000 °C of a cold deformed Nb-50(wt.)%Ti alloy. An ingot of the alloy was initially cast by the electron beam melting and remelting process and the cast ingot was next deformed by cold swaging. The evolution of microstructure and texture (in the macro, micro, and mesoscopic scales) during annealing was followed by optical microscopy, scanning electron microscopy (SEM), electron backscatter diffraction (EBSD), X-ray diffraction, and Vickers microhardness measurements.

2. Materials and methods

A compacted cylinder composed of a mixture of Nb machining chips and Ti sponge was melted in a 60 kW EBM furnace under vacuum (10^{-4} mbar). An excess of 2(wt.)% Ti was added to compensate for Ti loss by evaporation. After casting, the resulting ingot was remelted and cast again into a cylinder with 50 mm diameter and 200 mm length [14]. The chemical analysis of the cast alloy was: 49.9 ± 0.1 (wt.)%Ti, 800 ppm of O, 100 ppm of N, and 100 ppm of C. The content of interstitial elements meets the specifications for Nb-Ti superconducting alloys recommended by the ASTM B884–1 standard. Before cold deformation, the cast cylinder was machined into a bar of 38 mm diameter to fit into the swaging machine, remove surface irregularities, and eliminate a Ti-rich surface layer formed by condensation of Ti vapor. The machined bar was deformed by swaging at room temperature in three sequential deformation steps of area reductions 53.5%, 75.2%, and 89.5%. The final diameter was 12.3 mm [14]. Discs of about 5 mm thickness were cut from the transversal section of the bar and encapsulated in quartz ampoules under vacuum with a pressure of less than 5 10^{-2} mbar to avoid contamination with O and N from the atmosphere during the subsequent annealing cycles. The discs were then annealed during 1 h at temperatures of 250, 350, 500, 600, 750, 900, and 1000 °C.

Samples extracted from the discs before and after annealing were prepared by metallographic techniques for observation in both optical and scanning electron microscopes (SEM). The preparation steps were: (a) grinding with silicon carbide papers of 500, 600, 800, 1200, and 2000 grit sizes; (b) mechanical polishing with diamond pastes of 6 μm, 3 μm, and 1 μm; and (c) final mechanical polishing with a mixture of colloidal silica (0.05 μm) and hydrogen peroxide (10% by volume). The samples to be observed in the optical microscope were also etched in a solution of 3 HF: 5 HNO_3: 8H_2O for about 60 s. Before polishing with colloidal silica (after polishing with diamond past of 1 μm), Vickers microhardness measurements were made with a load of 2 N and X-ray diffraction patterns were obtained with CuKα radiation. The diffraction patterns were refined by the Rietveld method, with weighted profile residuals (Rwp) of approximately 10%. Macrotexture was also measured with X-ray diffraction (CuKα radiation) by the Schulz method [23]. The orientation distribution functions (ODF) were built from incomplete pole figures (α_{max} = 75°). The fiber macrotexture was extracted to section φ_2 = 0, ϕ = 45°, and φ_1 in the range of 0–90°. Microtexture and mesotexture were evaluated with the EBSD technique with a SEM.

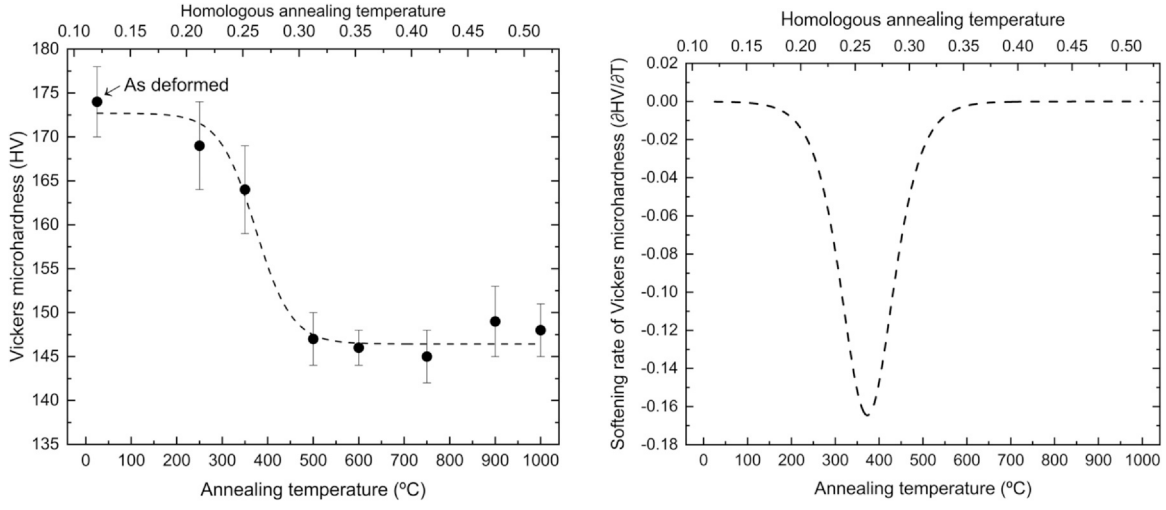

Fig. 1. Microhardness measurements (load of 2 N) of samples subjected to isochronous annealing cycles of 1 h: (a) Vickers microhardness and (b) softening rate as a function of the annealing and homologous annealing temperatures.

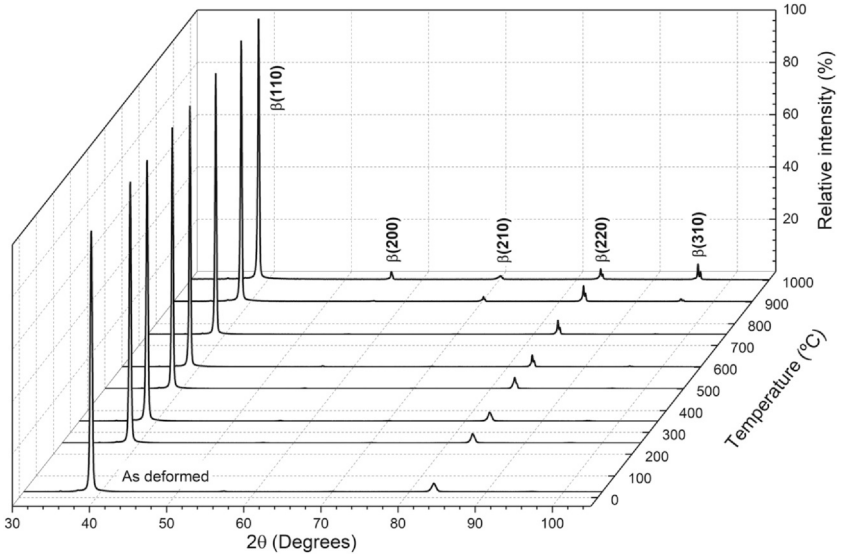

Fig. 2. Diffraction patterns (Cu-Kα radiation) of all samples of the Nb-50(wt.)%Ti alloy after cold swaging (as deformed) and after cold swaging and annealing at different temperatures for 1 h.

3. Results and discussion

3.1. Transformation followed by optical microscopy, X-ray diffraction, and microhardness measurements

The Vickers hardness measurements as a function of the annealing and homologous annealing temperatures are given in Fig. 1(a), showing a typical decrease (softening) when these temperatures increase. At 500 °C, the softening is practically complete and has probably been caused by recovery, as discussed later in this section. A sigmoid curve was adjusted to the experimental points and the softening rate was calculated as the derivative of this curve, which is given as a function of the annealing temperature in Fig. 1(b). The largest softening rate occurred at approximately 380 °C.

Microstructural modifications during annealing were investigated with X-ray diffraction and optical microscopy. The X-ray diffraction patterns of the cold deformed sample and of those deformed and annealed at different temperatures are given in Fig. 2. All patterns indicate a single phase of body centered cubic structure (β-phase; BCC) with a lattice parameter of approximately 0.3285 nm. The (220) peak of the β-phase is shown in detail in Fig. 3, where evidences of line sharpening and of the appearance of a Kα1 and Kα2 doublet are already seen at the annealing temperature of 500 °C, but these are well established at temperatures equal to or above 600 °C. In Fig. 4, the full-width at half-maximum (FWHM) of the peak is shown to decrease when the annealing temperature increases. Peak sharpening occurs when cold deformed metals are annealed, because of the rearrangement and elimination of crystalline defects (mainly dislocations) by recovery or recrystallization [24]. The main difference between these two modes of microstress reduction is that only during recrystallization does the elimination of defects occur by the migration of high-angle grain boundaries [25]. This distinction will be used later to identify the softening mechanism at different annealing temperatures.

Micrographs obtained with optical microscopy of the cold deformed alloy before annealing (Fig. 5) show evidences of deformation bands with curly morphology, especially in the central region of the bar cross section (Fig. 5b). This type of morphology often occurs in BCC metals and alloys deformed by swaging or drawing, but it has also been observed in FCC and HCP crystalline structures [16,17].

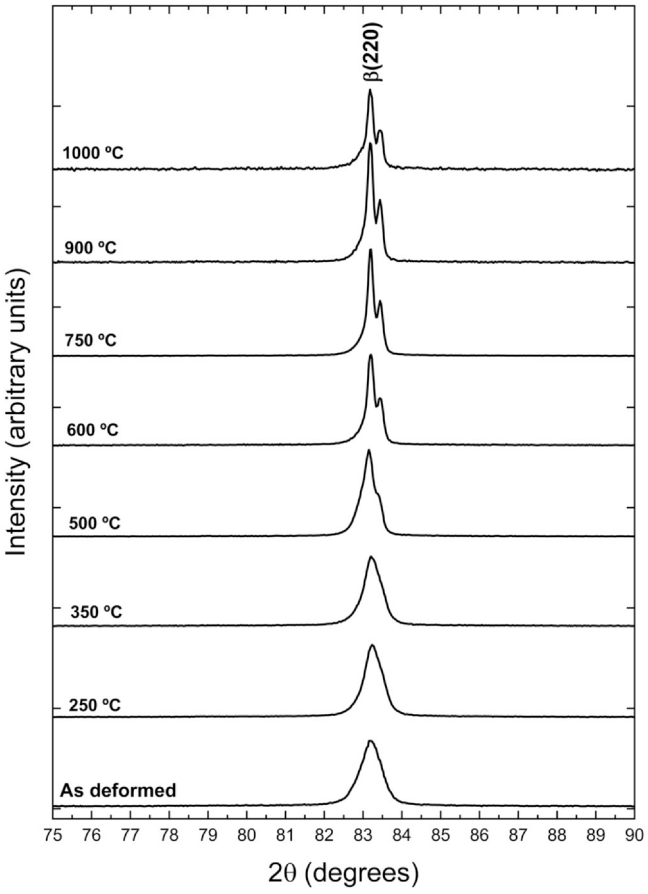

Fig. 3. Magnification of the (220) line of the β-phase observed in the diffraction patterns of Fig. 2.

After annealing at temperatures equal to or below 500 °C, the curly structure can still be seen (Fig. 6) without evidences of recrystallized grains and, consequently, of recrystallization. After annealing at 600 °C (Fig. 7), however, very few recrystallized grains

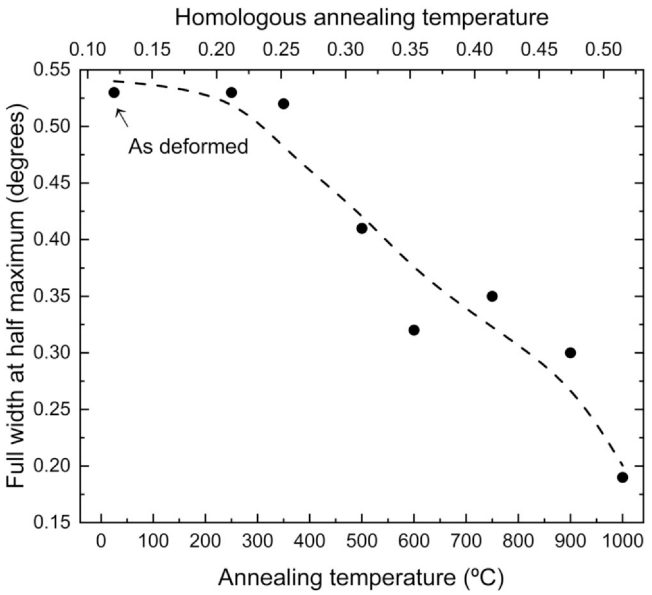

Fig. 4. Full-width at half-maximum of the (220) peak of the β-phase diffraction pattern as a function of the annealing temperature.

(confirmed by EBSD analysis) are indicated by arrows in Fig. 7(b), located within relatively large deformed grains of the curly structure. The absence of recrystallization after annealing at 500 °C and the incipient recrystallization after annealing at 600 °C imply that the substantial softening observed in Fig. 1 in the temperature range between 250 and 600 °C is due exclusively to recovery. This conclusion agrees with the significant softening by recovery reported in the literature for the annealing of cold worked BCC metals and alloys [22,26].

When the annealing temperature increases to 750 °C, recrystallized grains are now clearly visible (Fig. 8) and a further increase to 1000 °C causes not only extensive recrystallization, but also abnormal grain growth (Fig. 9). In this sample, the average grain size is 97 ± 11 μm, which is larger than the size of 36 ± 5 μm measured in the sample that was not annealed (Fig. 5), indicating that grain growth is significant at 1000 °C.

The volume fraction of recrystallized grains was measured by the manual counting procedure described in the ASTM E562–08 standard. A square grid of approximately 6000 points was used and the number of observed fields was sufficient to guarantee about 10% relative accuracy. The volume fraction of recrystallized grains is related to the annealing temperature in Fig. 10. Note that incipient recrystallization occurs at 600 °C, but the microstructure is completely recrystallized at annealing temperatures of 900 °C and 1000 °C, as observed in the micrographs. Consequently, the softening that occurred at these two temperatures might have been caused by a combination of recovery and recrystallization.

In the sample annealed at 1000 °C, it is still possible to see residues of the curly morphology underlying a completely recrystallized grain structure. The usual curly morphology is attributed to the dislocation substructure in the deformation bands [12,15], but deformation bands no longer exist in this sample after complete recrystallization. Therefore, the curly visual pattern still observed after annealing at 1000 °C is probably due to a microsegregation pattern that was originally formed during solidification of the cast ingot. An example of microsegregation in as-cast samples of a similar alloy has been reported in the literature [27]. This microsegregation was twisted during cold deformation by swaging and probably helped reveal the curly structure formed by deformation

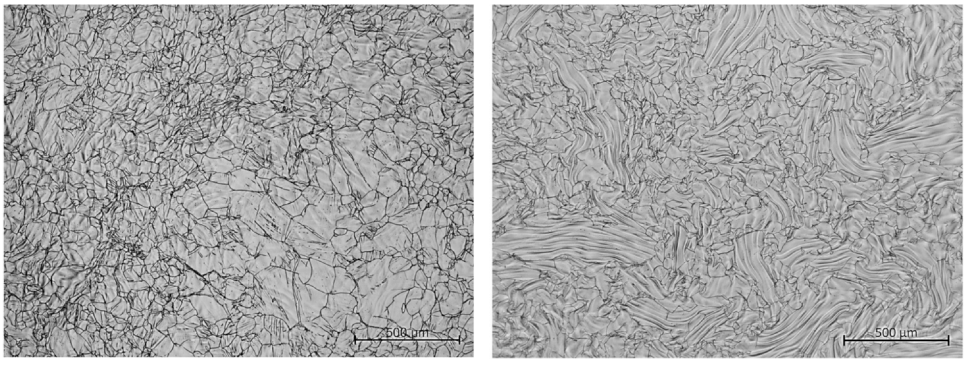

Fig. 5. Micrographs (optical microscopy) of cold swaged bar samples before annealing. Regions near the bar (a) surface and (b) center (etched with 3HF:5HNO_3:8H_2O for 60 s).

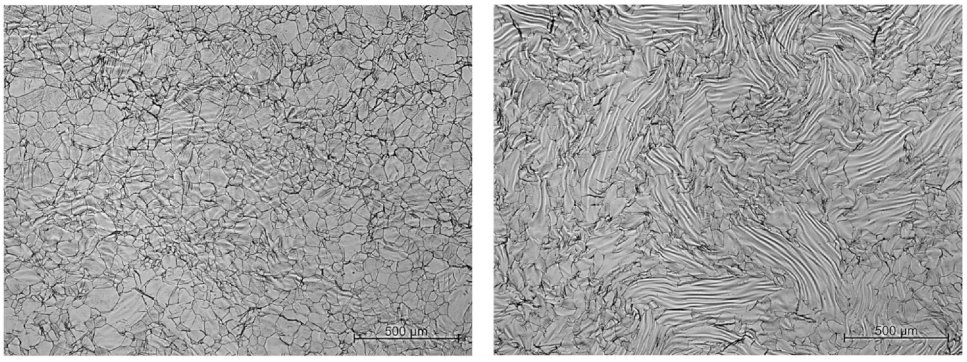

Fig. 6. Micrographs (optical microscopy) of samples of the cold swaged bar. Regions near the bar (a) surface and (b) center after annealing at 500 °C for 1 h (etching with 3HF:5HNO_3:8H_2O for 60 s).

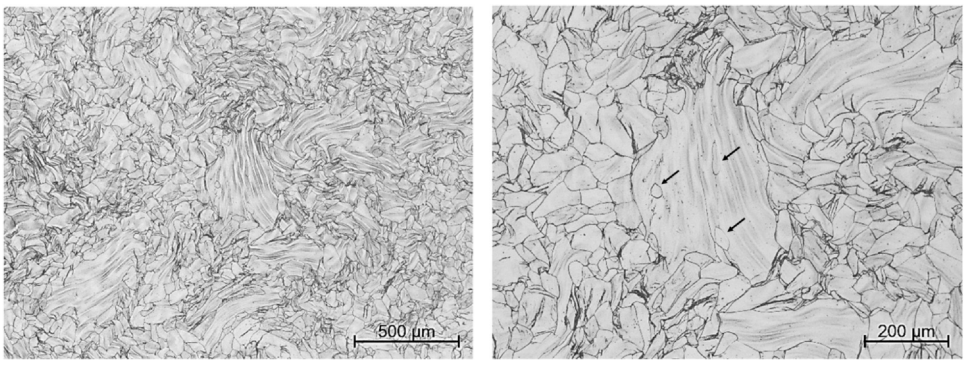

Fig. 7. Micrograph (optical microscopy) of a sample from (a) the central region of the cold swaged bar after annealing at 600 °C for 1 h and (b) a magnified view with very few recrystallized grains (indicated by arrows) within relatively large and deformed grains of the curly structure (etching with 3HF:5HNO_3:8H_2O for 60 s).

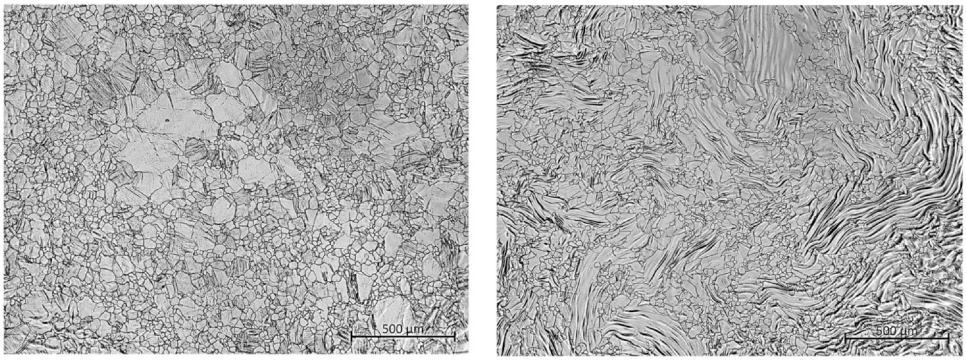

Fig. 8. Micrographs (optical microscopy) of samples of the cold swaged bar. Regions near the bar (a) surface and (b) center after annealing at 750 °C for 1 h (etching with 3HF:5HNO_3:8H_2O for 60 s).

bands after the samples were etched. Nevertheless, when recrystallization was complete, deformation bands were eliminated and only the microsegregation pattern remained in the form of the curly structure. Therefore, even after annealing at 1000 °C, the residual microsegregation was sufficient to be revealed by the etchant, showing a curly pattern. Note that recovery, recrystallization, and homogenization of composition are diffusion-controlled phenomena [28], but they occur by different mechanisms that have, respectively, increasing activation free-energy barriers. Therefore, as observed in the present work, increasing the annealing temperature would first promote recovery, then recrystallization, and finally composition homogenization.

3.2. Transformation followed by texture measurement

Maps of grain orientations were obtained by the EBSD technique for samples from the central region of the Nb-49.9% Ti bar after cold swaging (as deformed - AD) and after cold swaging and annealing at different temperatures (Fig. 11). The maps of the as-deformed sample and of those deformed and annealed at 250 or 600 °C have similar features, displaying gradients of orientations (gradients of colors) within grains. Relatively large deformed grains with internal color variations have parts with different orientations and, consequently, indicate a region not yet recrystallized [29,30]. Nevertheless, in the maps for the annealing temperatures of 750 or

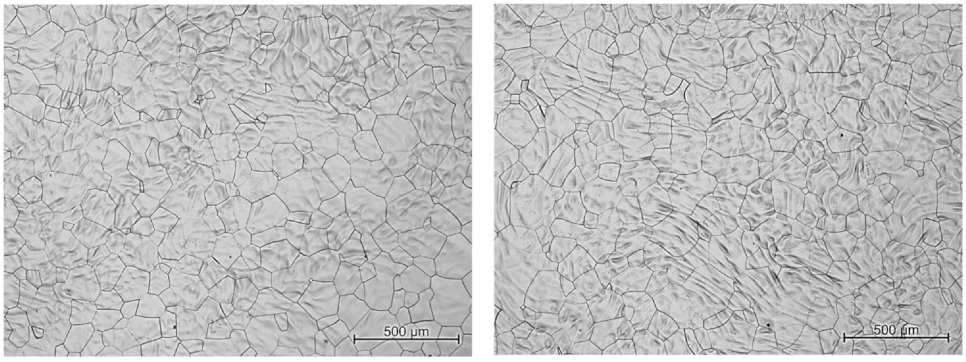

Fig. 9. Micrographs (optical microscopy) of samples of the cold swaged bar. Regions near the bar (a) surface and (b) center after annealing at 1000 °C for 1 h (etching with 3HF:5HNO_3:8H_2O for 60 s).

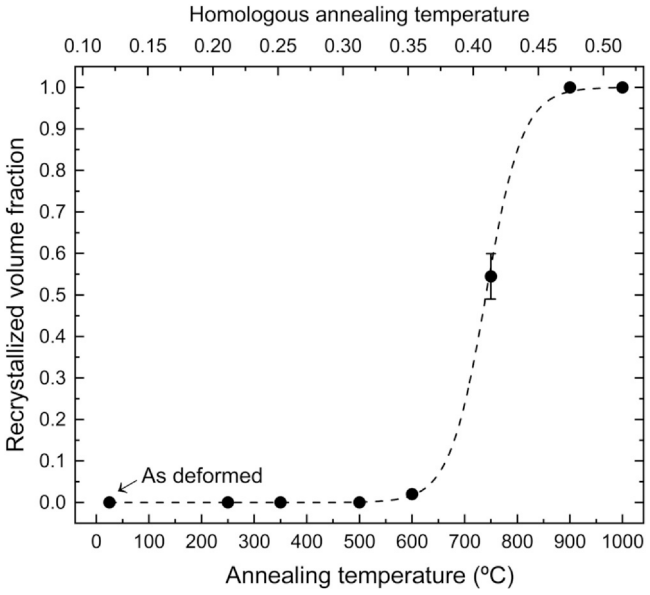

Fig. 10. Recrystallized volume fraction as a function of the temperature and homologous temperature of isochronous annealing cycles of 1 h.

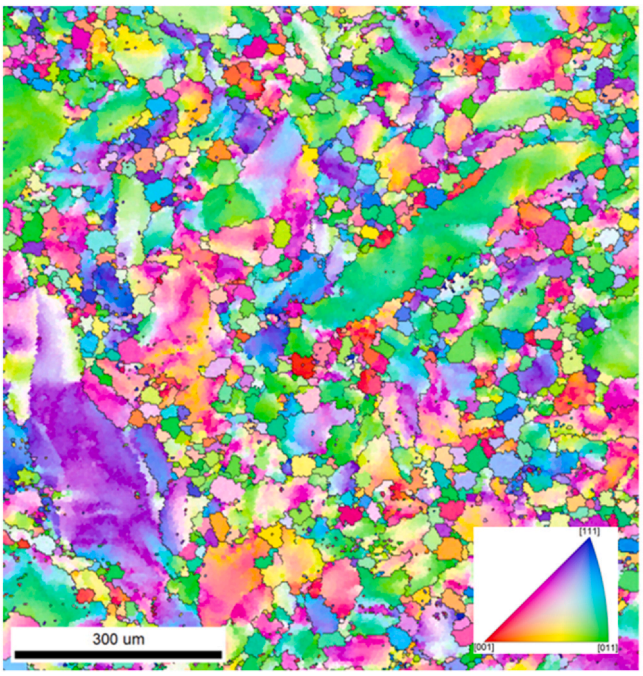

Fig. 12. Electron backscatter diffraction (EBSD) map showing a partially recrystallized microstructure in the sample from a central region of the bar, deformed by cold swaging and annealed at 750 °C for 1 h. Different colors represent different crystallographic orientations, indicated in the inverse pole figure.

1000 °C, recrystallized grains with uniform orientations (uniform colors) exist, confirming that recrystallization occurred significantly at these temperatures. Recrystallization occurred in approximately 50% of the volume of the sample annealed at 750 °C, as indicated by the many relatively small grains with uniform colors shown in detail in Fig. 12. In the map for the annealing temperature of 1000 °C, completely recrystallized grains (uniform internal colors) have grown extensively throughout the sample.

Maps of the distribution of grain boundary misorientations for the same microstructures of Fig. 11 are provided in Fig. 13. There is no significant difference in the distributions of low-angle, high

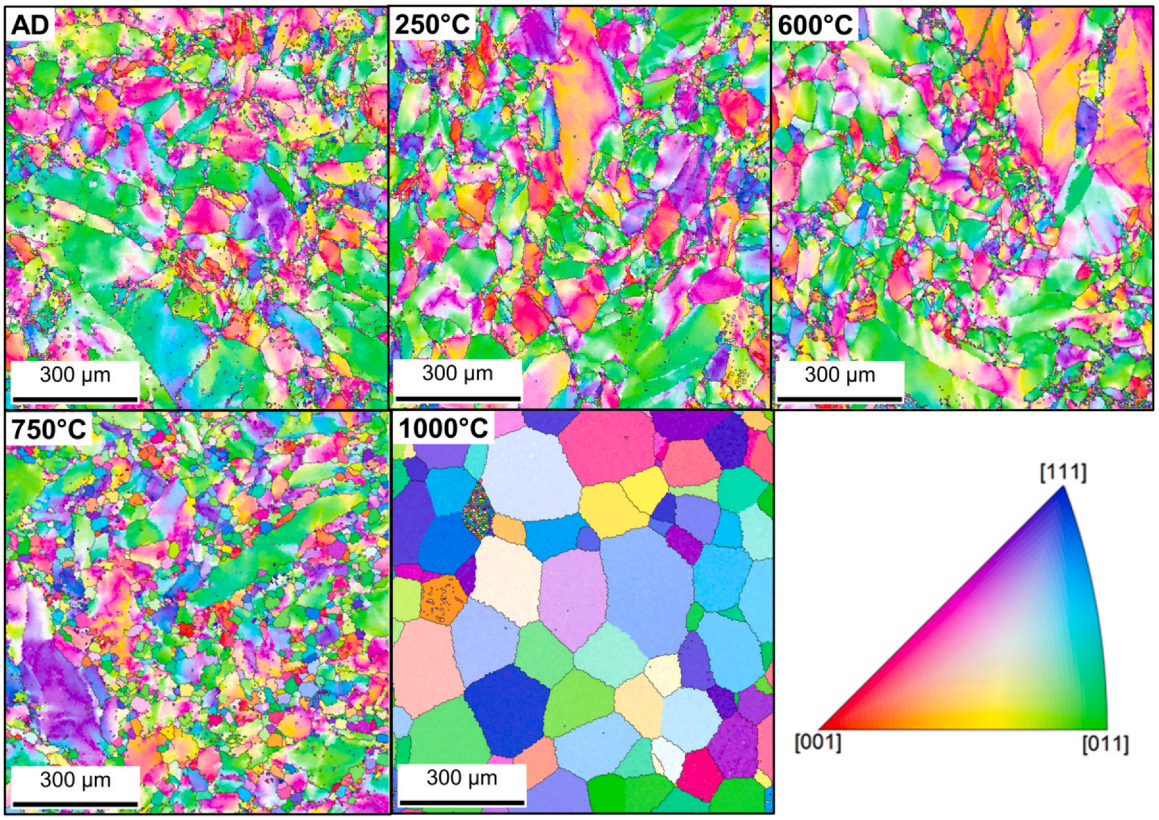

Fig. 11. Electron backscatter diffraction (EBSD) maps of samples from the central region of the Nb-49.9% Ti bar after cold swaging (as deformed - AD) and after cold swaging and annealing at the indicated temperatures for 1 h. Different colors represent different crystallographic orientations indicated in the inverse pole figure at the lower-right side.

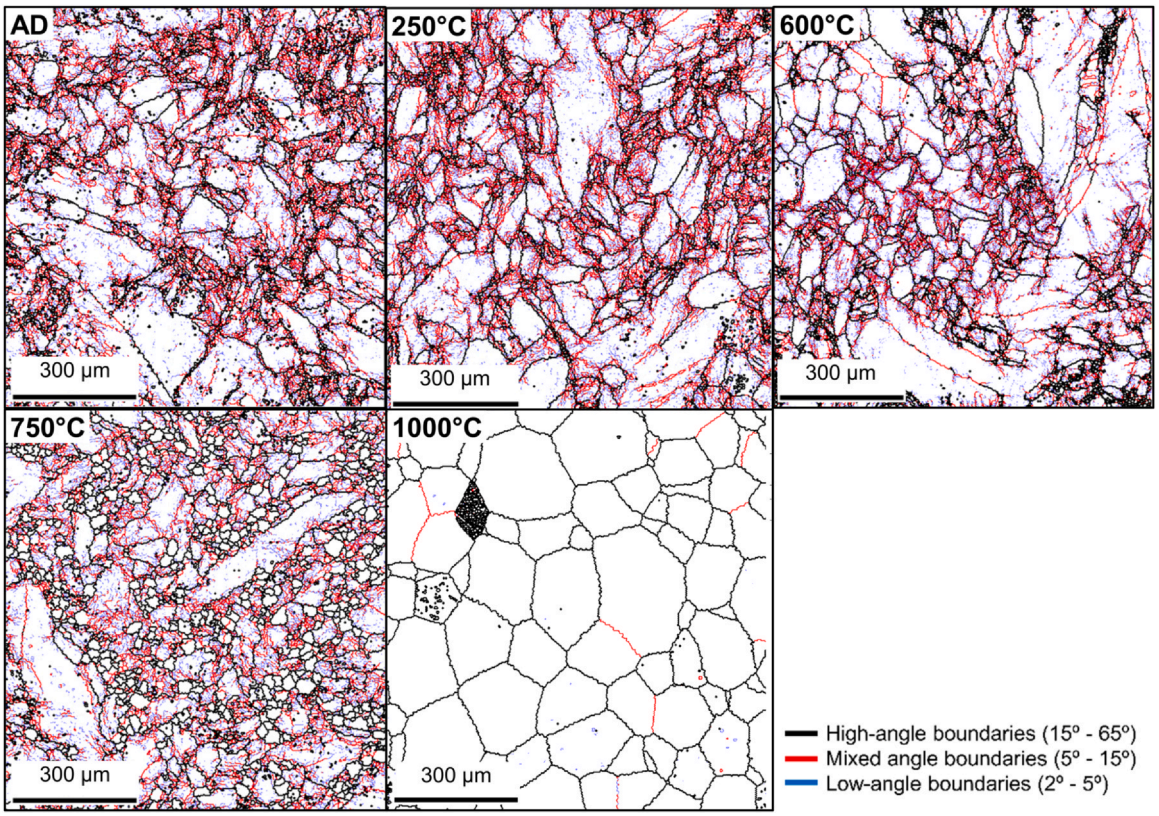

Fig. 13. Maps of distribution of grain boundary misorientations of samples from the central region of the Nb-49.9% Ti bar after cold swaging (as deformed - AD) and after cold swaging and annealing at the indicated temperatures for 1 h.

angle, and mixed-angle boundaries between the map of the as-deformed sample and those of the samples deformed and annealed at 250 or 600 °C, which is consistent with the maps of Fig. 11. Low and mixed-angle boundaries suggesting the existence of cell/subgrain boundaries are observed within grains, which are outlined by high-angle boundaries. In the map for the annealing temperature of 750 °C, given in detail in Fig. 14, relatively small recrystallized grains without cell/subgrain boundaries are noted. In the annealing temperature of 1000 °C, boundaries are mainly high-angle, since the low and mixed-angle boundaries were eliminated by complete recrystallization.

The recovery and recrystallization events that were confirmed by complementary characterization techniques suggest that the samples deformed by sequential steps of area reductions of 53.5%, 75.2%, and 89.5% and subsequently annealed for 1 h in the temperature range between 500 and 600 °C could display improved superconducting properties. The present experimental evidence indicate that these samples might have a well-defined structure of subgrains, because they have undergone significant recovery without recrystallization. As mentioned in the introduction section, subgrain boundaries work as flux pinning centers, which improve the superconducting properties [19,25]. This improvement for the suggested conditions, however, should be verified with further experiments.

In the cold deformed sample and also in those samples subsequently annealed, the orientation distribution functions (ODF) indicate a fiber texture, in which the planes (110) are scattered at random in directions perpendicular to the < 110 > direction, which is parallel to the swaging direction (Fig. 15). This texture, reported in the literature [31] for deformed metals, agrees with models proposed to explain the formation of the curly structure [16,17].

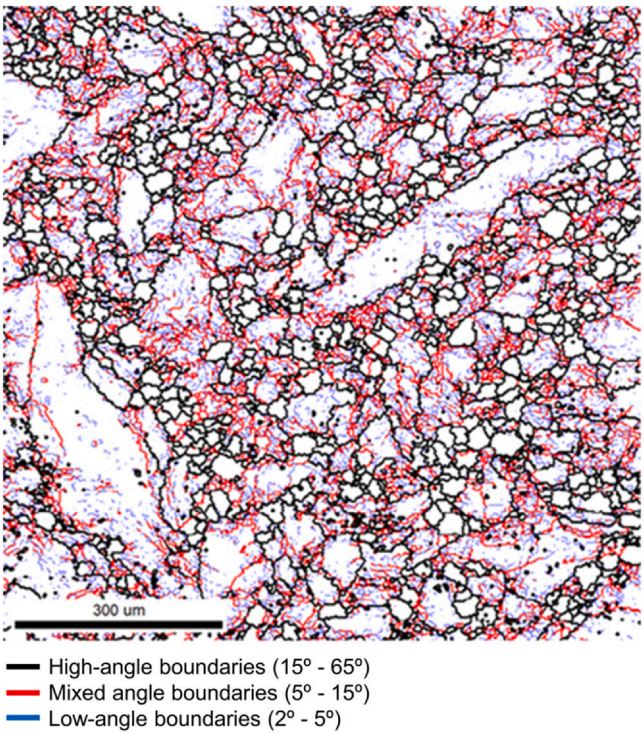

Fig. 14. Map of grain boundary misorientations showing the distribution of recrystallized grains and subgrains of the Nb-49.9% Ti bar after cold swaging and annealing at 750 °C for 1 h. Central region of bar.

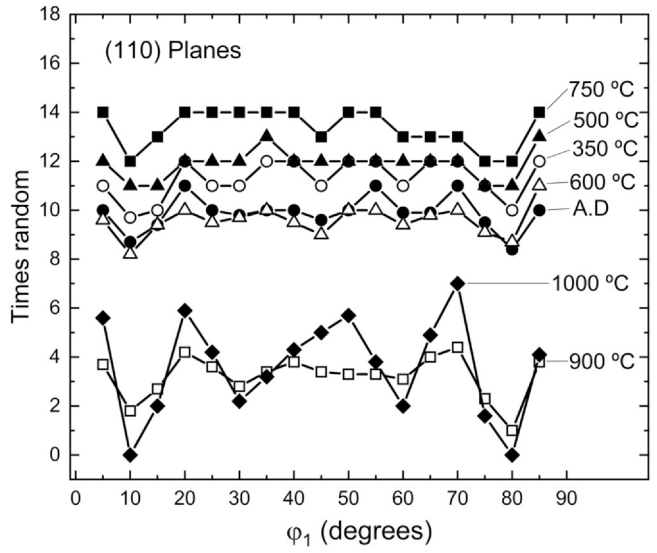

Fig. 15. Fiber texture in the cold deformed sample (as deformed - A.D) and in the samples annealed at different temperatures. The fibers appear in the transversal section and were extracted from the ODF with section of $\varphi^2 = 0$ and $\phi = 45°$.

For the annealing temperatures in the range between 250 °C and 500 °C, only recovery occurred, and for 600 °C or 750 °C, recrystallization was negligible or only partial, respectively. Consequently, the fiber texture in these annealed samples were practically similar to that in the cold deformed sample (and not annealed), because recovery does not change crystallographic orientations significantly. In the samples annealed at 900 °C and 1000 °C, however, complete recrystallization was observed, clearly reducing the intensity of the fiber texture because of the significant rearrangement of crystal planes that occurred within the recrystallized grains.

4. Conclusions

An ingot of a Nb-49.9(wt.)%Ti alloy, cast after electron beam melting and remelting, was deformed into a bar by cold swaging. Different slices of this bar were subsequently annealed for 1 h (isochronous annealing) at different temperatures in the range between 250 and 1000 °C. The X-ray diffraction patterns of all samples (cold deformed with or without subsequent annealing) indicate the presence of only the β-phase, with a body-centered cubic structure (BCC). In the samples annealed at temperatures up to 600 °C, since recrystallized grains are not detected or are negligible, recovery is the main mechanism of softening, which was observed by microhardness measurements. After annealing at 750 °C, however, approximately 50% of the sample volume consists of recrystallized grains (confirmed by EBSD). At the temperatures of 900 °C and 1000 °C, recrystallization occurs completely and might contribute to softening. Some grain growth is also noted at 1000 °C. Observations with the optical microscope of the cold deformed sample (not annealed) and of the samples with subsequent annealing at temperatures up to 600 °C reveal a “curly structure”, which is a visual pattern attributed to deformation bands and their dislocation substructures. In the samples annealed at 900 °C and 1000 °C, however, deformation bands are eliminated by recrystallization, but the curly pattern still exists and is now probably due to a residual microsegregation of elements that formed during solidification of the initial cast ingot. A fiber texture is observed in the cold deformed sample and in the samples annealed at temperatures up to 750 °C. After annealing at the temperatures of 900 °C and 1000 °C, the intensity of the fiber texture significantly decreases owing to complete recrystallization.

Funding

This work was supported by CAPES-Brazil.

CRediT authorship contribution statement

Andrei Marx Ferreira: Conceptualization, Data curation, Formal analysis, Investigation, Methodology, Project administration, Resources, Software, Visualization, Roles/Writing – original draft, Writing – review & editing. **Marcelo Aquino Martorano:** Formal analysis, Visualization, Roles/Writing – original draft, Writing – review & editing. **Nelson Batista de Lima:** Formal analysis, Investigation, Methodology, Validation, Visualization, Writing – review & editing. **Angelo Fernando Padilha:** Conceptualization, Funding acquisition, Methodology, Project administration, Resources, Supervision, Writing – original draft.

Declaration of Competing Interest

The authors declare that they have no known competing financial interests or personal relationships that could have appeared to influence the work reported in this paper.

Acknowledgements

One of the authors (AMF) thanks CAPES-Brazil for the scholarship.

References

[1] D.L. Grigsby. Niobium alloys and compounds, Air Force Materials Laboratory, USA, EPIC Report DS-148, January 28, 1966.
[2] R.M. Scanlan, A.P. Malozemoff, D.C. Larbalestier, Superconducting materials for large scale applications, Proc. IEEE 92 (10) (2004) 1639–1654, https://doi.org/10.1109/JPROC.2004.833673
[3] M.S. Lubell. State-of-the art of superconducting magnets, Oak Ridge National Laboratory (ORNL), USA, Report ORNL-TM 3921, September 1972.
[4] A. Cremasco, W.R. Osório, C.M.A. Freire, A. Garcia, R. Caram, Electrochemical corrosion behavior of a Ti-35Nb alloy for medical prostheses, Electrochim. Acta 53 (14) (2008) 4867–4874, https://doi.org/10.1016/j.electacta.2008.02.011
[5] S. Barannikova, G. Schlyakhova, O. Maslova, Y. Li, Z. Lev, Fine structural characterization of the elements of a Nb-Ti superconducting cable, J. Mater. Res. Technol. 8 (1) (2019) 323–332, https://doi.org/10.1016/j.jmrt.2018.02.004
[6] M. Fischer, D. Joguet, G. Robin, L. Peltier, P. Laheurte, In situ elaboration of a binary Ti-26Nb alloy by selective laser melting of elemental titanium and niobium mixed powders, Mater. Sci. Eng. C 62 (2016) 852–859, https://doi.org/10.1016/j.msec.2016.02.033
[7] J.M. McKinnell: Flux pinning in superconducting Nb-Ti alloys. Ph.D. thesis, University of Wisconsin-Madison, USA, 1990.
[8] B.L. Pereira, C.M. Lepienski, V. Seba, G. Hobold, P. Soares, B.S. Chee, P.A.B. Kuroda, E.S. Szameitat, L.L. Santos, C.R. Grandini, M. Nugent, Titanium-niobium (Ti-xNb) alloys with high Nb amounts for applications in biomaterials, Mater. Res. 23 (6) (2020).
[9] M.T. Naus, R.W. Heussner, A.A. Squitieri, D.C. Larbalestier, High field flux pinning and the upper critical field of Nb-Ti superconductors, IEEE Trans. Appl. Supercond. 7 (2) (1997) 1122–1125, https://doi.org/10.1109/77.620688
[10] J.L. Murray, The Nb-Ti (Niobium-Titanium) system, Bull. Alloy Phase Diagr. 2 (1) (1981) 55–61.
[11] D. Pattanayak, B. Obst, U. Wolfstieg, Röntgenographische phasenbestimmung an niob-titan-supraleitern, Z. Metallkd. 72 (7) (1981) 481–486, https://doi.org/10.1515/ijmr-1981-720705
[12] I. Pfeiffer, H. Hillmann, Der Einfluss der Struktur auf die Supraleitungseigenschaften von NbTi 50 und NbTi 65, Acta Metall. 16 (12) (1968) 1429–1439, https://doi.org/10.1016/0001-6160(68)90038-2
[13] H. Albert, I. Pfeiffer, Erratum: Borderud SP, Li Y, Burkhalter JE, Sheffer CE and Ostroff JS. Electronic cigarette use among patients with cancer: characteristics of electronic cigarette users and their smoking cessation outcomes. Cancer. doi: 10.1002/ cncr.28811, Cancer 121 (3) (2015) 800, https://doi.org/10.1002/andp.19384240505
[14] J.C. Petoilho: Recristalização das ligas supercondutoras do sistema Nb-Ti. Doctorate Thesis, Faculdade de Engenharia, University of Campinas (Unicamp), São Paulo, Brazil, 1986.
[15] P.J. Lee, D.C. Larbalestier, Niobium-titanium superconducting wires: nanostructures by extrusion and wire drawing, Wire J. Int. 36 (2) (2003) 61–66.
[16] W.F. Hosford, Microstructural changes during deformation of [011] fibre-textured metals, Trans. Metall. Soc. AIME 230 (1) (1964) 12–15.

[17] J. Gil Sevillano, C. García-Rosales, J. Flaquer Fuster, Texture and large–strain deformation microstructure, Philos. Trans. R. Soc. A 357 (1756) (1999) 1603–1619, https://doi.org/10.1098/rsta.1999.0392
[18] A.W. West, D.C. Larbalestier, Microstructural changes produced in a multifilamentary Nb-Ti composite by cold work and heat treatment, Metall. Trans. A 15A (1984) 843–852.
[19] D. Dew-Hughes, T. Luhman, Treatise on Materials Science & Technology: Metallurgy of Superconducting Materials, Elsevier Inc, New York, 1979.
[20] A.M. Campbell, J.E. Evetts, Flux vortices and transport currents in type II superconductors, Adv. Phys. 21 (90) (1972) 199–428, https://doi.org/10.1080/00018737200101288
[21] M. Pohl, H. Dinkler, A.F. Padilha, F. Heisterkamp, Metallographische Untersuchungen an einer supraleitenden Legierung aus Nb-47Ti, Sonderbd. Prakt. Metallogr. 19 (1988) 319–326.
[22] H.P. Stüwe, A.F. Padilha, F. Siciliano Jr., Competition between recovery and recrystallization, Mater. Sci. Eng. A 333A (2002) 361–369, https://doi.org/10.1016/S0921-5093(01)01860-3
[23] Satyam Suwas, Ranjit Kumar Ray, Crystallographic Texture of Materials, Springer, London, 2014.
[24] B.D. Cullity, Elements of X-Ray Diffraction, second edition, Addison-Wesley, 1978, pp. 285–292.
[25] A. Rollett, F. Humphreys, G.S. Rohrer, M. Hatherly, Recrystallization and Related Annealing Phenomena, second ed., Pergamon Press, Oxford, 2004.
[26] F. Siciliano Jr., W.A. Monteiro, A.F. Padilha, Comparative study of the recrystallization of pure niobium and Nb-1 wt% Zr, Z. Metallkd. 86 (10) (1995) 713–718, https://doi.org/10.1515/ijmr-1995-861010
[27] W.Q. Wei, H.W. Wang, Z.X. Gao, Z.J. Wei, Microstructure evolution of as-cast Nb-Ti-C alloys, Trans. Nonferrous Met. Soc. China 19 (2009) 440–443, https://doi.org/10.1016/S1003-6326(10)60085-4
[28] J.W. Martin, R.D. Doherty, Stability of Microstructure in Metallic Systems, Cambridge University Press, Cambridge, 1976.
[29] V. Randle, O. Engler, Texture Analysis, Gordon Breach Science Publishers, Amsterdam, 2000.
[30] V. Randle, Electron backscatter diffraction: strategies for reliable data acquisition and processing, Mater. Charact. 60 (9) (2009) 913–922.
[31] D.T. Read, Metallurgical effects in niobium-titanium alloys, Cryogenics 18 (10) (1978) 579–584, https://doi.org/10.1016/0011-2275(78)90184-4